ACTA IMEKO
ISSN: 2221-870X
June 2025, Volume 14, Number 2, 1 - 11

Investigating the sufficient measurement distance for a UAV-performed VHF/UHF radiation pattern measurements

Jakub Krchnák[1], Michal Dzuriš[1], René Harťanský[1], Ján Halgoš[1], Anatolii Kliuchka[1], Michal Štibraný[2]

[1] *Institute of Electrical Engineering FEI STU, Bratislava, Slovakia*
[2] *MWTC, s. r. o., Trenčianska Teplá, Slovakia*

ABSTRACT
The transmission of radio signals in VHF and UHF frequency bands is facilitated by large antenna systems situated at high altitudes and considerable heights above the ground. To determine the functionality of such systems, a crucial procedure is radiation pattern measurement, especially before and after replacing old antennas with new ones. Advancements in drone technology offer a possibility of employing semi-autonomous drones to perform the radiation pattern measurement, providing a high measurement flexibility. Due to the broad spectrum of capabilities offered by drones, compared to the previously used helicopters, there is a need to reevaluate the established method of radiation pattern measurement in the context of drone-based measurements. This study focuses on the analysis of the amplitude errors caused by the quadratic phase error resulting from wavefront curvature in finite-distance radiation pattern measurements. The article presents horizontal and vertical radiation patterns of antenna systems of different sizes and topologies, calculated using the computational software Altair FEKO. Deviations from the radiation patterns calculated for the ideal case of infinite distance are discussed. Additionally, the calculated vertical radiation patterns are compared to those obtained from measurements performed using a commercially available quadcopter and a specialized measurement device.

Section: RESEARCH PAPER

Keywords: Antenna measurements; numerical simulation; UAV; radiation pattern

Citation: J. Krchnák, M. Dzuriš, R. Hartanský, J. Halgoš, A. Kliuchka, M. Štibraný, Investigating the sufficient measurement distance for a UAV-performed VHF/UHF radiation pattern measurements, Acta IMEKO, vol. 14 (2025) no. 2, pp. 1-11. DOI: 10.21014/actaimeko.v14i2.2066

Section Editor: Luca Callegaro, INRiM, Italy

Received February 1, 2025; **In final form** May 28, 2025; **Published** June 2025

Funding: This work was supported by the grant agency APVV under a project number APVV-20-0042 “Microelectromechanical sensors with radio frequency data transmission” and by the project: ENEFS 09I05-03-V02-00041 "Novel electrically enhanced wireless method for sensing of mechanical quantities".

Corresponding author: Jakub Krchnák, e-mail: jakub.krchnak@stuba.sk

1. INTRODUCTION

Terrestrial broadcasting of FM (Frequency Modulated) and DVB-T (Digital Video Broadcast - Terrestrial) radio signals is realized by large antenna systems (AS) situated at high altitudes, such as hilltops. To achieve the desired radiation pattern and signal coverage, antenna systems are placed on towers or antenna masts at significant heights above the ground surface. Currently, there is an ongoing replacement of these antenna systems, and to ensure the new AS retains the properties of the old AS, its parameters must be reviewed. One of the fundamental parameters describing the function of the AS is its radiation pattern. Various methodologies have been employed to measure the radiation pattern of antennas [1]–[3]; however, for antenna systems used in terrestrial broadcasting, airborne evaluation is the only feasible measurement method. Previously, this measurement was carried out by helicopters equipped with specialized measurement equipment and a trained crew [4]. Advances in Unmanned Aerial Vehicle (UAV) technology now allow semi-autonomous quadcopters to replace helicopters, providing better measurement variety. Quadcopters can perform similar flights to helicopters but are much cheaper to maintain (or rent), can take off from any area with sufficient clearance, and can perform more delicate measurements much closer to the Antenna Under Test (AUT/AS). Moreover, their smaller size and composite material structure minimize possible sources of measurement error previously introduced by the large reflective hulls of helicopters.

Many studies have already utilized UAVs for antenna measurements over a broad spectrum of frequencies from VHF/UHF [5]–[7] to several GHz [8]–[10]. For measuring the AS radiation patterns in this study, a UAV would adopt a similar methodology to a helicopter, such as circular flights in the

horizontal plane, vertical flights, and possibly propagation flights, while maintaining the advantage of flying significantly closer to the AS. However, flying closer to the AS introduces the issue of measurement error caused by the quadratic phase error at finite distances [11]. The sufficient distance for radiation pattern measurement, where the deviation caused by quadratic phase error is acceptably small, has already been a topic of study for various antenna arrays and apertures. The well-known Rayleigh criterion:

$$r_1 \geq \frac{2D^2}{\lambda}, \tag{1}$$

where:

r - is the distance from Antenna Under Test (AUT),
D - is the largest dimension of the AUT,
λ - is the operating wavelength,

has been investigated. Studies [12], [13] have shown that the sidelobe level and the aperture distribution affect the distance requirement. These studies proved the (1) requirement insufficient and proposed a measurement distance ranging from $6\ D^2/\lambda$ to $16\ D^2/\lambda$. On the contrary, [14] has shown that $2\ D^2/\lambda$ may be too strict, and the measurement error may be acceptable even at smaller distances for certain EM field distributions across the antenna array.

Current radiation pattern measurements are performed according to the reports ITU-R SM.2056 – Airborne Verifications of Antenna Patterns of Broadcasting Stations [15] and RA11 – Antenna Measurements in VHF and UHF Frequency Bands [11] in Slovakia, which are primarily proposed for measurements with helicopters. Both reports state that the minimum sufficient measurement distance for far-field pattern evaluation is (1) and recommend a measurement distance of at least 1 km. However, the aforementioned studies [12]–[14] question this distance criterion, presenting results that either require larger distances or allow smaller ones, respectively. It can be expected that different sufficient measurement distances are required for different sized antenna systems. Additionally, [11] specifies only the measurement distance for an AS with an electrical size larger than $10\ \lambda$ but does not offer an alternative for a smaller system. The largest FM antenna systems in Slovakia do not reach such sizes. Given this variability and the technical specifications of UAVs, the focus of this study is on evaluating the minimum sufficient distance at which the phase error caused by wavefront curvature results in deviations small enough to be negligible for real measurements.

Section 2 specifies the utilized methods. Calculation method using the computational software Altair FEKO and numerical antenna substitution is described, as well as the considered measurement method utilizing a UAV.

Section 3 presents the calculated radiation patterns in FEKO at various finite distances for FM antenna systems of different sizes and topologies. These patterns are compared to those calculated for an observation point at an infinite distance and deviations are considered for several key features of interest. Calculated vertical radiation patterns at certain distances are compared to previously obtained vertical radiation patterns measured at similar distances to the calculations.

The article concludes with stating general equations to determine the minimal radiation pattern observation distance for tested antenna systems, a brief discussion of the presented results and offers suggestions for future research and analysis.

2. METHODS AND PROCEDURES

Sufficient measurement distance can be determined using various methods, the most logical being by performing measurements at different distances. However, to reliably evaluate the amplitude errors caused by finite-distance observations would require an extensive amount of radiation pattern measurements for each AS individually. Furthermore, outdoor measurements can be affected by factors such as ground reflections and scattering or weather conditions which would make the evaluation ineffective and impossible to create a general criterion. There is also a possibility of carrying out measurements in an anechoic chamber, which eliminates weather effects and most of the surrounding environment factors, however, antenna systems for terrestrial broadcasting at VHF and UHF frequency bands can be as large as 20 – 30 m and cannot be dismounted from the antenna mast. Hence, the only possibility to evaluate the radiation pattern at various distances for multiple antenna systems is to utilize numerical calculations. For these calculations, the computational software Altair FEKO can be used. FEKO offers a capability to create a parametric model of the real antenna and, based on an aperture current distribution, is able to calculate the electromagnetic field (EMF) scattered by the antenna [16]. Furthermore, FEKO can substitute the parametric model with a numerical representation. This substitution is a spherical array of Hertzian Dipoles with a radius similar to the distance at which the EMF was calculated [16]. This process is illustrated in Figure 1a. The array can replicate the EMF at a defined distance (radius), and calculations at further distances utilize the numerical substitution instead of the parametric model [17]. The numerical representation will be further referred to as Hertzian Dipole Structure (HDS). This allows for simplified calculations and is especially advantageous when more than one antenna needs to be defined for calculations, as is the case with the AS. Due to the complexity of the real antenna structure, it is impossible to calculate the radiation pattern of the AS comprised of parametric models on commonly available hardware. Using the HDS, it is possible to create numerical representations of the AS. Antenna systems for terrestrial FM and DVB-T signal broadcasting usually consist of similar antenna types for multiple antenna systems. Therefore, by calculating the radiation of only a small number of different parametric models (antenna types), and subsequently replacing them with HDSs, it is feasible to create numerical representations of large number of antenna systems, offering a greater number of samples for evaluation. HDSs must be spaced out, and their amplitudes and phases have to be adjusted according to the technical documentation provided by the AS operator. Figure 1b - Figure 1d display the AS representations in FEKO comprised of different number of similar antennas, replaced by the HDSs. The AS in Figure 1b represents the AS consisted of

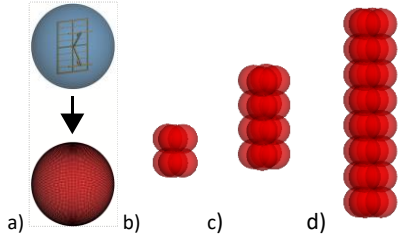

Figure 1. Parametric antenna model substitution by a) HDS, b) AS comprised of 6 HDS, c) AS comprised of 16 HDS, d) AS comprised of 32 HDS.

6 antennas distributed in 3 azimuths and 2 levels and is 5.69 m in height. The AS in Figure 1 represents the AS consisting of 16 antennas distributed in 4 azimuths and 4 levels. This AS is 12.1 m in height and the AS in Figure 1d represents the AS consisting of 32 antennas distributed in 4 azimuths and 8 levels with 24.89 m in height. Antenna systems with similar topology represent most of the currently operating ones in Slovakia.

2.1. Radiation pattern generated by HDS

The HDS can replicate the radiation of a single antenna in both the near-field and far-field as well as the AS radiation pattern in the far-field. Due to the nature of HDS, however, it is important to test if this approach can estimate the behaviour of the EMF even at closer distances to the AS and as such serve as a basis for defining a sufficient measurement distance. An antenna array created from parametric models of the antennas can serve as a reference for comparisons. Due to the aforementioned complexity of the FM antennas, for this purpose, an array of patch antennas at higher frequencies can be utilized. The advantage of utilizing the patch antennas for this test besides their simple geometry, is their comparable radiation pattern to FM antennas. Therefore, it is possible to achieve a radiation pattern similar to that of the FM antenna system. Figure 2 displays the antenna arrays used for the investigation. Figure 2a shows an array of four parametric models of patch antennas situated above each other, in order to produce a desired pattern in the vertical plane. Figure 2b shows the same array, in this case, however, parametric models are replaced with HDSs.

The objective is to determine the distance at which the finite-distance radiation pattern converges to the ideal infinite-distance pattern, ensuring that the largest amplitude error does not exceed a certain value. Additionally, the study aims to assess whether this determined distance is similar for both cases – parametric models and HDSs. Differences of radiation pattern can be presented as a function of distance, position and amplitude.

Figure 3a displays the far-field radiation pattern in the vertical plane facilitated by the array of parametric models (displayed in Figure 2a) and by an array of HDSs (displayed in Figure 2b). Slight differences can be observed at the local maxima of the four side lobes. These patterns are used as a reference for comparisons with finite-distance patterns respectively. Relations of the amplitude error with respect to the distance from the antenna array are displayed in Figure 3b for parametric models and Figure 3c for HDSs. At first look, these plots appear similar, therefore, based on these density plots and scientific literature, the maxima of four sidelobes were chosen for a closer inspection due to their susceptibility to error caused by insufficient measurement distance. These points at local

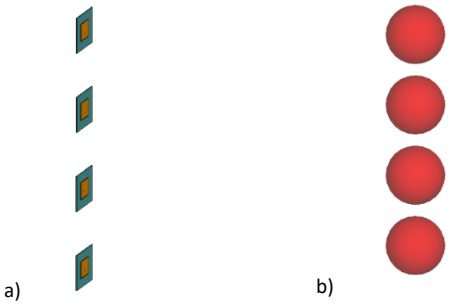

Figure 2: a) Substitute scaled AS consisted of patch antenna parametric models, b) substitute AS consisted of HDS substitutes for patch antennas.

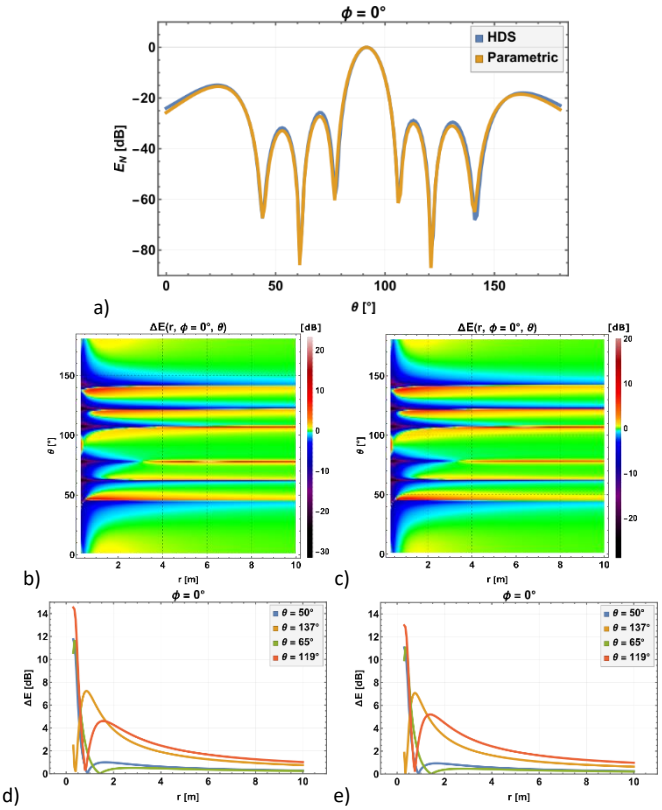

Figure 3: a) Far-field vertical patterns of the substitute AS generated by parametric models (orange) and HDS (blue), b) values of amplitude error for parametric substitute AS, c) values of amplitude error for numeric substitute AS, d) values of amplitude error at specific points for parametric model, e) values of amplitude error at specific points for numeric model.

maxima display the differences between the respective far-fields. The error magnitudes are displayed in Figure 3d and Figure 3e. Slight differences can again be observed at an immediate distance from the antenna array – meaning that the radiation pattern behaves differently at very close distances in the case of parametric models and HDSs. However, in these regions, the error magnitude is also increasing, which means that the radiation pattern changes significantly in shape – the radiation pattern is still forming and the sidelobes can shift in position as well as the main lobe beamwidth is subject to change. This region should be avoided when considering radiation pattern measurements and considered should be only distances greater than the closest possible distance at which all the displayed curves are declining. This occurs first at approximately 2.5 m. If the level of 2 dB is chosen as the maximum allowed error, all the curves reach or are smaller than this value at the distance of 4.5 m. At and beyond this distance, the curves in both Figure 3d and Figure 3e have similar values. Since the maximum allowed amplitude error is in the report [11] defined at 0.5 dB, this level is significantly below the 2 dB threshold and the method of distance investigation using the HDS can be considered valid. The method was tested for horizontal patterns as well, yielding similar results. Hence, this method can be applied to FM antenna systems.

2.2. Measurement setup and procedure

Before the calculation method can be applied to FM antenna systems, it is important to define the measurement procedure and setup in order to determine restrictions imposed on the measurement that have to be taken into account during final

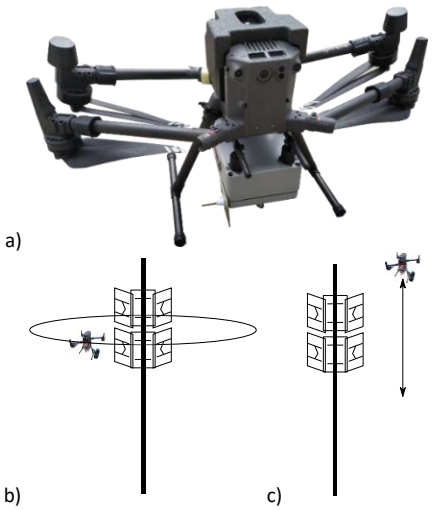

Figure 4: Proposed measurement setup – a) DJI Matrice 300 + Pixla 1, b) illustration of circular horizontal flight, c) illustration of vertical flight.

considerations. The proposed measurement procedure follows the standard airborne radiation pattern measurement proposed for helicopters. In this study, the procedure involves an autonomous UAV, *DJI Matrice 300* (instead of a helicopter), with a specialized measurement device, *Pixla 1*, developed by the authors [1]. This measurement setup is displayed in Figure 4a. The quadcopter can semi-autonomously carry out the predefined mission by following waypoints defined by the pilot. However, to perform the mission, the quadcopter must maintain a connection with the device operated by the pilot on the ground. If the connection is lost, either due to substantial foliage coverage or geological/artificial obstructions, the quadcopter returns to the point of take-off. To obtain the radiation pattern projection in principal planes, the quadcopter can perform circular (horizontal) and vertical flights. During the circular flight, the quadcopter follows a path around the AS while maintaining the constant distance and altitude, but rotates, in order to always keep the measurement antenna in a position to measure the tangential part of the incident EMF. Using the setup in Figure 4a, the quadcopter has to always face the AS. The circular flight is illustrated in Figure 4b. The vertical flight is performed at a constant distance and azimuth. The quadcopter takes the position at a desired azimuth, distance and in altitude lower than the altitude of the geometrical centre of the AS. Subsequently, the quadcopter ascends to the altitude significantly higher than the AS centre. The vertical flight illustration is displayed in Figure 4c. During the flight the quadcopter, utilizing the RTK (Real-Time Kinematic Positioning) records data about its position, time and its own tilt, while *Pixla 1* records the EMF intensity data. After the measurements are done, data is sorted, and the radiation pattern is synthesized [5]. Before flights can be carried out, several guidelines and restrictions have to be defined.

Original guidelines for an airborne measurement dictate three major restrictions regarding the measurement distance which are determined by the physical properties of the AS and technical capabilities of an airborne vehicle [11]. First restriction (r_1) is defined by Rayleigh distance (1) and this is the criterion that is investigated within this study. Second restriction (r_2) adheres to the capability of the airborne vehicle – UAV to maintain the desired altitude and the tilt of the main lobe (α). It has been standardized that the deviation from the desired altitude should not exceed the boundaries defined by the angle

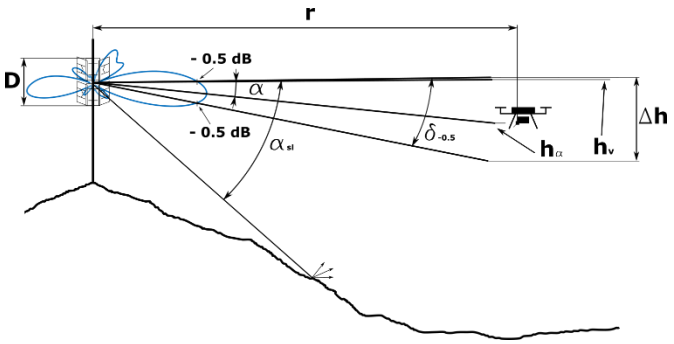

Figure 5: Illustration of airborne radiation pattern measurement.

between two points on the main lobe, attenuated by 0.5 dB against the main lobe maximum. Based on the main lobe tilt applies:

$$r_2 \geq \frac{\Delta h}{\tan\left[\frac{\delta_{-0.5dB}}{2} + \alpha\right] + \tan\left[\frac{\delta_{-0.5dB}}{2} - \alpha\right]}, \quad (2)$$

where:

Δh - is the UAV altitude uncertainty,

$\delta_{-0.5dB}$ - is the angle between two points on the main lobe attenuated by 0.5 dB compared to the radiation maximum.

α - is the main lobe tilt angle,

for $\alpha \leq \delta_{-0.5dB}/2$.

And:

$$r_2 \geq \frac{\Delta h}{\tan\left[\alpha + \frac{\delta_{-0.5dB}}{2}\right] - \tan\left[\alpha - \frac{\delta_{-0.5dB}}{2}\right]} \quad (3)$$

for $\alpha > \delta_{-0.5dB}/2$.

Thanks to the use of RTK and PPK (Post-Processed Kinematic Positioning) technology utilized by the *DJI Matrice 300,* the quadcopter is capable of positioning uncertainty $\pm$ 0.5 m in all axes.

The third criterion (r_3) is given by the capability of the UAV to maintain a constant distance from the AS. The report [11] states that the distance deviation caused by the positioning error cannot exceed 5.5 % of the measurement distance. Taking into consideration the quadcopter positioning capability the minimal distance to satisfy this condition is 18.18 m. All these criteria must be satisfied and can be summarized as:

$$(r \geq r_1) \wedge (r \geq r_2) \wedge (r \geq r_3). \quad (4)$$

The measurement distance (mainly for horizontal pattern measurements) can be further specified by performing a propagation flight. During the propagation flight, the quadcopter takes a position at a measurement altitude and at a large distance from the AS. Subsequently, the quadcopter executes an approach, while maintaining a constant altitude. The region where the local minima and maxima of the propagation flight measurements are closest together is then selected as appropriate [15]. The region of the ground-reflected EM waves can be also estimated by the main lobe tilt and angle of the adjacent sidelobes (α_{sl}). The flight altitude (h_α) is determined based on the altitude of geometrical centre of the AS (h_v) and the main lobe tilt. The illustration of the airborne measurement is displayed in Figure 5.

One other criterion exists that only applies to quadcopter and is crucial when choosing the measurement distance, especially for horizontal flight. And it is the flight time for one set of batteries. This time is determined by the batteries themselves and the payload. The EMF intensity measurement device "Pixla 1" weighs ~3 kg. With this type of payload, the quadcopter *DJI Matrice 300* can remain in the air for approximately 25 minutes, that includes also the time for safe return to the point of take-off. The flight speed must also be chosen with care since higher speed means bigger quadcopter tilt. Bigger quadcopter tilt, which based on the measurement antenna, introduces bigger polarisation loses and therefore introduces unnecessary systematic error into the measurement. If we consider the maximum flight speed of 4 m s^{-1}, the quadcopter can perform a circular flight with radius of 954 m. However, also the distance to and back from the starting point has to be considered and this reduces the flight radius to 724.4 m. It is also necessary to presume that quadcopter will not maintain a maximum speed throughout the entire flight and also has to stop at the starting point of the flight to position itself. Moreover, environmental conditions such as wind speed can influence the flight, hence, to ensure the safe return to the take-off point, the circular flight radius should not exceed 500 m. This defines the fourth restriction (r_4):

$$r \leq r_4. \tag{5}$$

This criterion strictly adheres to the type of UAV in use as well as the type of payload. Lowering the payload weight (using a smaller measurement device) will increase the flight time and will allow larger radii for circular flight.

3. FM ANTENNA SYSTEM RADIATION PATTERNS

Having established a calculation method, an evaluation procedure and defined the guidelines posed by a measurement procedure, the investigation can be applied to the FM antenna systems. The reference (the ideal case of fully formed radiation pattern that does not change with distance and only plane wave exists [18]) can be established by calculating the radiation pattern at infinite distance in two principal planes.

Figure 6 displays the far-field radiation patterns in horizontal and vertical planes of the three FM antenna systems from the Figure 1. Figure 6a and Figure 6d shows horizontal and vertical patterns of the AS in Figure 1b, Figure 6b and Figure 6e shows horizontal and vertical patterns of the AS in Figure 1c and Figure 6c and Figure 6f display horizontal and vertical patterns of the AS in Figure 1d. Vertical patterns are always displayed in the direction of maximum radiation (main lobes) which for the AS shown in this study constitutes azimuths $\varphi = 330°$, $\varphi = 345°$ and $\varphi = 70°$. The shape of vertical patterns is largely similar across a larger number of antenna systems in Slovakia based on the number of levels meaning antenna systems with similar number of antenna levels, and subsequently size, have very similar vertical pattern. Certain deviations, such as main lobe tilt or side lobe attenuation result from a specific placement or slight variations in topology based on the structural capabilities and demands of the operator, however, the number of sidelobes remains largely the same. This fact allows a generalization of the method presented in this study. Horizontal patterns are usually specifically tailored to the needed coverage in the area.

3.1. FM antenna system radiation pattern at finite distances

The criterion that is widely utilized for a lower far-field (Fraunhoffer region) boundary is a Rayleigh criterion (1) and is based on a maximum acceptable quadratic phase error caused by the wavefront curvature. Based on the previous investigation [19] a phase difference of 22.5°, resulting from a larger distance to the edge of the antenna array compared to the distance to the geometrical centre of the array, produces the resulting amplitude error in the measurement of gain of 0.1 dB. From the Pythagorean theorem a following equation can be derived:

$$(r_1 + \Delta r)^2 = r_1^2 + \left(\frac{D}{2}\right)^2, \tag{6}$$

where:

r - is the distance from the geometrical centre of the AS,
D - is the largest dimension of the AS.

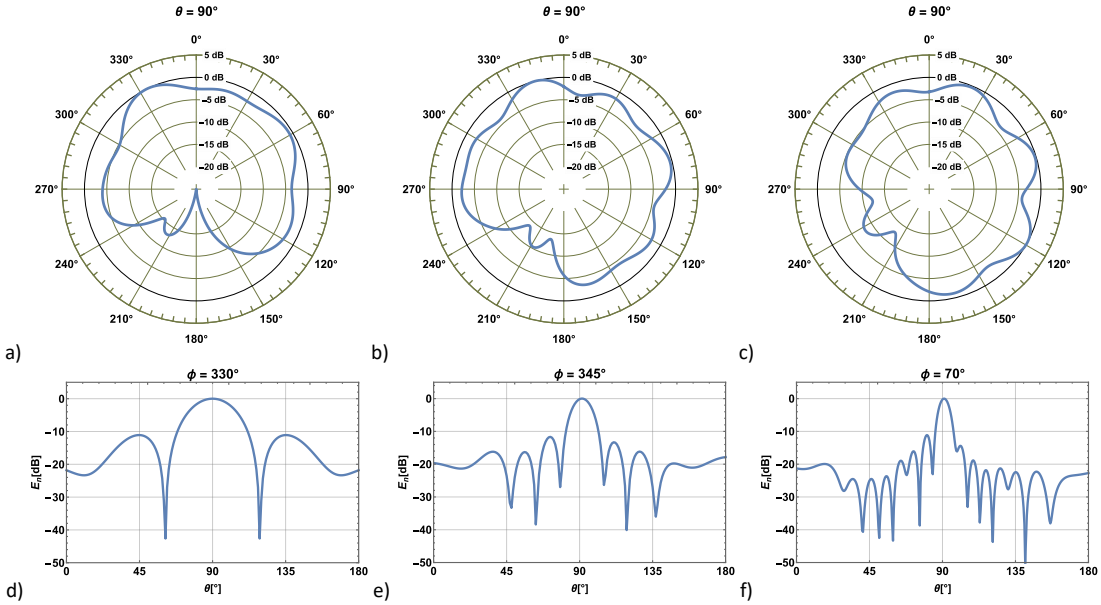

Figure 6: a) Horizontal and d) vertical pattern of the AS in Figure 1b, b) horizontal and e) vertical pattern of the AS in Figure 1c, c) horizontal and f) vertical patterns of the AS in Figure 1d.

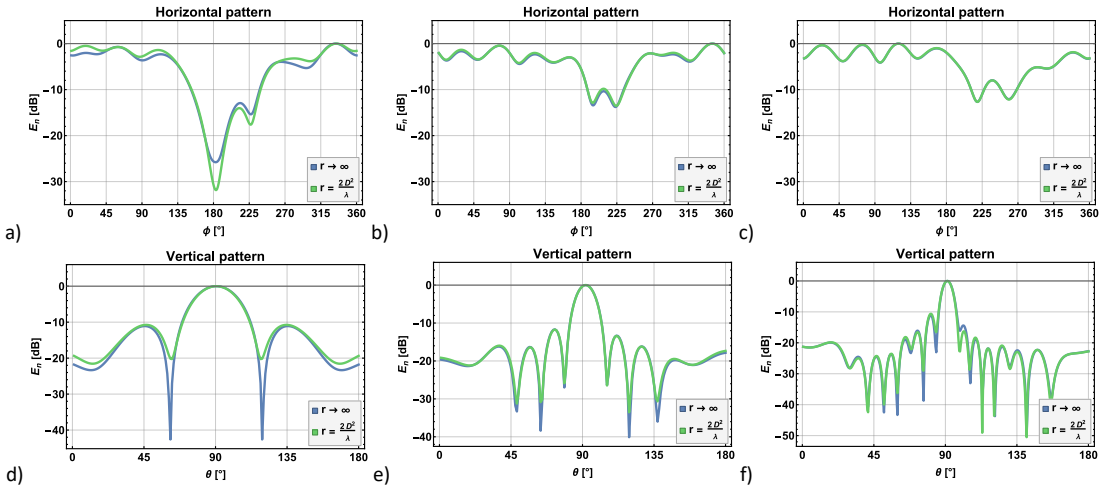

Figure 7: Comparisons of ideal far-field patterns with patterns at (1): a) horizontal and d) vertical for the AS in Figure 1b, b) horizontal and e) vertical for the AS in Figure 1c, c) horizontal and f) vertical for the AS in Figure 1d.

Subsequently, (2) can be adjusted for *r*:

$$r = \frac{D^2}{8\,\Delta r} - \frac{\Delta r}{2}, \tag{7}$$

and if $\Delta r \ll r, \Delta r \ll D$ (3) reduces to:

$$r_1 = \frac{D^2}{8\,\Delta r}. \tag{8}$$

From (4), (1) can be obtained by setting $\Delta r = \lambda_0/16$, which equals 22.5°. First distance at which radiation patterns are calculated is defined by (1) to determine if, for the three investigated antenna systems, this distance is sufficient. Resulting distances are 20.7 m for the AS in Figure 1b further referred to as a *small AS*, 97.7 m for the AS in Figure 1c further referred to as a *medium AS* and 378.6 m for the AS in Figure 1d further referred to as a *large AS*. These designations are based on their individual electrical sizes and serve only for differentiation and classification of the antenna systems in this study. Otherwise, all the antenna systems used in the FM frequency band are known as large ones.

Radiation patterns in the principal planes at the distance (1) are displayed and compared with ideal patterns in Figure 7. The *small AS* horizontal patterns (Figure 7a) show visible differences not only in minima dividing the main lobes, but in the lobes themselves. The largest amplitude error in the horizontal pattern occurs at approximately 180°. This error occurs at the global minimum of the radiation pattern. Since the exact value at the minima is not as important as the values of the maxima in the FM antenna system radiation pattern measurements, attention should be directed to the main radiation lobes. Absolute amplitude errors (up to 1.5 dB) can be observed in this region of the main radiation as well. This points at distance (1) being insufficient for horizontal radiation pattern measurements as the amplitude error values exceed the desired 0.5 dB level. Similar case occurs in Figure 7d which shows significant disparities between vertical patterns of the *small AS*. Figure 7b displays the horizontal pattern of the *medium AS* (Figure 1c) and in this case there is a good agreement between finite distance and ideal patterns with only negligible values of the amplitude error. Vertical patterns in Figure 7e also show a good agreement and differ only in minima between sidelobes. As was already stated, the minima are not as important for outside airborne measurements and, therefore, for this *medium AS* the (1) can be considered sufficient. Horizontal patterns of the *large AS* in Figure 7c are identical while vertical patterns in Figure 7f differentiate. Besides minima between sidelobes there is also notable amplitude error in the small sidelobe adjacent to the main lobe. This confirms conclusions reached by [12] and [13], hence, (1) is insufficient for *large AS* vertical pattern observations. On the other hand, for the horizontal pattern observation, the distance (1) is starting to approach the maximal circular flight radius distances (r_4) specified in the last section. This means that only one circular flight between the battery exchanges can be performed or based on the surroundings foliage can cause obstructions that may lead to the loss of connection and subsequently to the interruption of the flight. Given that the two displayed patterns are identical, there may be a smaller distance (flight radius) at which the 0.5 dB error level criterion is satisfied, making the measurement procedure more manageable.

3.2. Evaluation

Possible points of interest that can be investigated to determine the sufficient measurement distance are the maxima of individual lobes, as these are the most important in determining the sufficient coverage. This fact is especially important when considering the horizontal radiation pattern. However, since radiation patterns of FM/DVB-T antenna systems for the most part does not have highly attenuated minima, even small deviations in these local minima dividing the lobes can cause unification of adjacent lobes and appear as one larger lobe instead. Furthermore, this phenomenon would be the most debilitating factor during the AS diagnostics by radiation pattern measurements [19]. Such effects manifest in Figure 7a. It is therefore advantageous to display the value of the amplitude error as a function of angle and distance, similar to the case in Section 2. The distance plots displaying the values of amplitude error for the horizontal and vertical patterns from Figure 6 are displayed in Figure 8. Mutual differences (amplitude errors) of the ideal and finite distance patterns are displayed at distances from 15 – 500 m.

Figure 8a and Figure 8b represent the amplitude error values for the patterns in Figure 7a and Figure 7d (*small AS*). For the horizontal patterns (Figure 8a) visible error values appear at azimuths ~20°, ~100° and ~290° which are two main lobes and one region between lobes corresponding to local minimum in the ideal pattern. The largest deviations, however, occur at azimuths ~185° and ~230° which are located in the region of

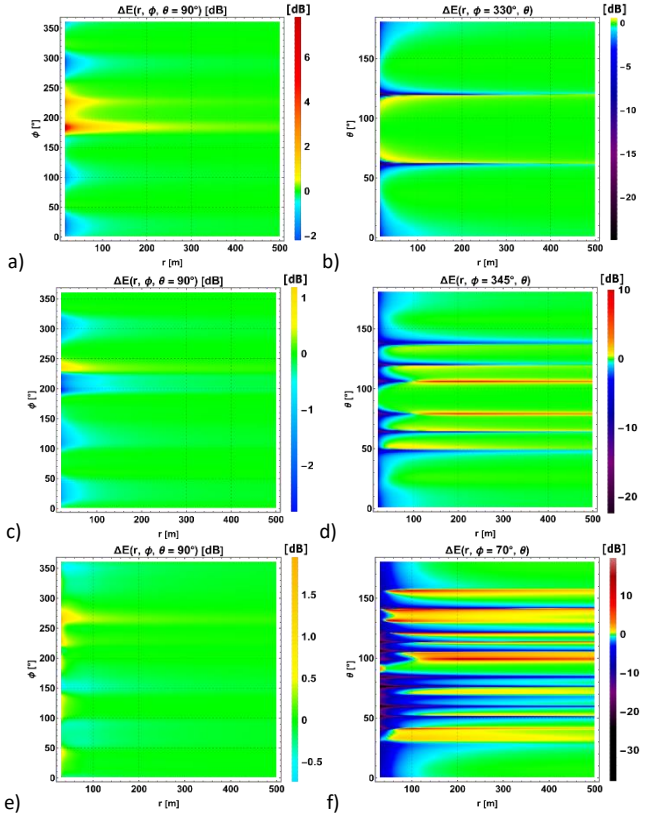

Figure 8: Amplitude error values as a function of distance and angle for: a) small AS horizontal pattern, b) small AS vertical pattern, c) medium AS horizontal pattern, d) medium AS vertical pattern, e) large AS horizontal pattern, f) large AS vertical pattern.

larger attenuation. These regions even experience larger attenuation at finite distances than in the ideal pattern. This behaviour of attenuated regions also corresponds to the previous research in this topic [20]. Even though these are the regions of largest disparity, as was already mentioned, for the purposes of airborne measurements, the region of main radiation is the main region of interest. Hence, specific points of interest are chosen from this region. For vertical patterns (Figure 8d), largest deviations, preserving even at the distance of 500 m are again located at global minima, however, even the two sidelobes and the main lobe experience visible deviations. Thus, two points at the main lobe and sidelobes appear appropriate for further investigation.

Figure 8c displays the amplitude errors for the horizontal pattern of the *medium AS* (Figure 6b) which is in terms of physical dimensions larger. Noticeable amplitude errors are visible in this case as well: in the main direction of radiation, specifically at azimuths ~25°, ~110°, ~310°. Again, the largest deviations appear in the region of attenuation at azimuth ~200°. However, in this case the pattern settles at a shorter distance than in the previous case (*small AS*). This phenomenon is caused by smaller values of attenuation where the global minimum is at value - 14 dB, whereas in previous case the global minimum reaches -32 dB. Vertical pattern differences for *medium AS* in Figure 6d display larger deviations at highly attenuated minima prevailing at large distances. This is the recurring occurrence for all highly attenuated minima, which are present in larger quantities in vertical patterns (see Figure 6). This pattern closely resembles the pattern created by the patch antennas and similarly the main point of interest will be the maxima of four sidelobes.

Figure 8e displays the values of amplitude error for the horizontal pattern of the *large AS*. In this case the deviation values appear to diminish at shorter distances compared to the previous cases, even though, in terms of physical size this AS is more than twice as large as the *medium AS*. This directly opposes the "rule of thumb" practice that the sufficient measurement distance increases with AS dimensions. The *large AS* vertical pattern deviations are displayed in Figure 8f and appear the most articulated. That is due to the large number of sidelobes and subsequently large number of highly attenuated minima. In this case the four sidelobes adjacent to the main lobe will be the main points of interest due to their susceptibility to quadratic phase error and measurement at insufficient distance can cause them to unify with the main lobe or appear unreasonably attenuated.

3.3. Finite radiation pattern measurement distance specification

Based on plots in Figure 8 and measurement considerations for the *small AS* horizontal pattern, several azimuths were chosen to display the value of amplitude error as a function of distance. These azimuths are 20°, 60°, 100°, 290°, 332° which are located at lobe maxima or in regions between the lobes that experience the largest deviations. Four elevation angles that experience the largest deviations (excluding highly attenuated minima) were chosen. These elevation angles are 30°, 70°, 115°, 150°. Graphs displaying the amplitude error values are displayed in Figure 9a – horizontal pattern, and Figure 9b – vertical pattern. The minimal allowed error value of 0.5 dB is marked and the sufficient measurement distance is determined at the point where the deviation values at all azimuths/elevation angles are equal or smaller than this threshold. Amplitude error values at all azimuths (Figure 9a) cross or remain below the threshold at the distance of approximately 75 m. At this distance, the value of quadratic phase error (ψ), calculated using (4)-(6), is 6.2°. This value is significantly lower than the Rayleigh distance phase error of 22.5°. Amplitude error values at all

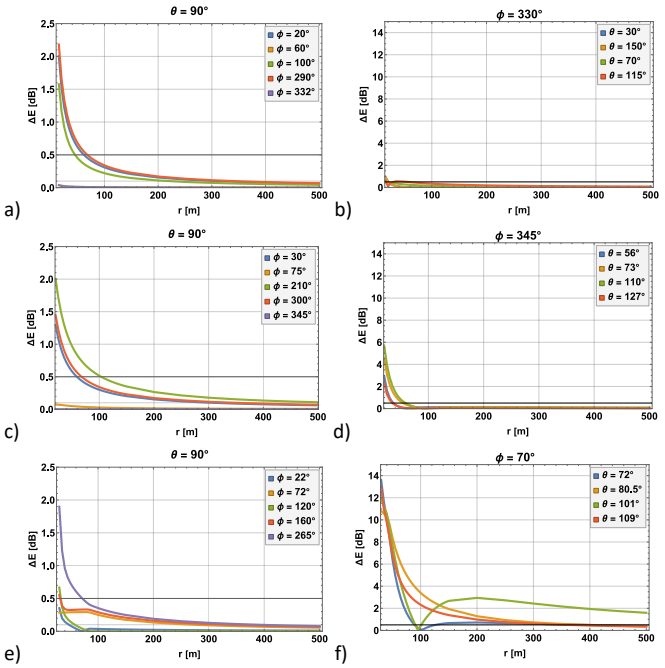

Figure 9: Amplitude error values at specific points as a function of distance and angle for: a) small AS horizontal pattern, b) small AS vertical pattern, c) medium AS horizontal pattern, d) medium AS vertical pattern, e) large AS horizontal pattern, f) large AS vertical pattern.

elevation angles (Figure 9b) cross the maximum allowed error value at the distance 55 m and the value of $\psi = 8.5°$. A similar procedure (using azimuths and elevation angles unique to the tested AS) was used for the other two antenna systems (their patterns) with *medium AS* (Figure 9c and Figure 9d) measurement distances being $r_{1h} = 105$ m | $\psi = 20{,}9°$ for the horizontal pattern and $r_{1v} = 55$ m | $\psi = 40{,}0°$ for the vertical pattern. The *large AS* presents a unique case, where for the horizontal pattern error values in Figure 9e are lower than the maximum allowed error at approximately 65 m. However, the character of the change shows that all the curves start to decline only at a distance of 85 m. As mentioned in Section 2, only distances at which all deviations are declining should be considered, since at that point the radiation pattern shape resembles the far-field pattern shape with only different values of normalized pattern at maxima and minima. If this condition is not satisfied, even though the deviation values at specific points are lower than the maximum allowed error threshold, overall observation error is much more significant due to the positions of minima and maxima shifting in space as well as the value. The amplitude error characteristics for the vertical pattern present no less interesting case. The Figure 9f shows that the amplitude error value at the elevation angle 101° does not cross the maximum allowed error value in the tested distance range. This point corresponds to the maximum of the small sidelobe adjacent to the main lobe. The deviation at this point satisfies the 0.5 dB threshold at the distance of 1 750 m, with a quadratic phase error value of 4.9°. This distance is significantly larger than the one defined by (1) and approaches the values of ψ presented in [12]. Such a large disparity suggests that horizontal and vertical pattern observations may need to be conducted separately during measurement.

4. RESULTS AND DISCUSSION

The investigation in the previous section puts the widely used Rayleigh distance requirement into question, however, offers inconclusive results. In one case, (1) is not sufficient enough, while in another other, this criterion seems too strict and potentially complicates radiation pattern measurement. Hence, it appears necessary to test the presented methodology on a larger number of antenna systems. In total, eight antenna systems were tested utilizing the methodology presented in this study.

These antenna systems are listed in Table 1. Seven of which operate in FM frequency band, and one – in DVB-T frequency band. Based on their physical size relative to the wavelength they are divided in three categories – small, medium and large similarly to the three antenna systems presented in previous sections which are listed in the table as AS1, AS5, AS7. All the tested FM antenna systems have similar gap between antennas in neighbouring levels, hence, different AS sizes are only determined by the number of antenna levels (i.e., the number of antennas vertically). Antennas in one level are rotated in different azimuths, the number of antennas in each level and their rotation is determined by the desired radiation pattern.

The determined distances at which the maximum error value (0.5 dB) is satisfied are listed in Table 2 along with their respective quadratic phase errors for both horizontal and vertical pattern observation – distinguished by the lower indices. In the Table 2 are also listed distance criteria specified in Section 2, where r_2 is defined by the quadcopter capabilities and the main lobe beamwidth in the vertical pattern, while r_3 and r_4 are solely defined by the quadcopter capabilities. All these criteria can vary based on the utilized UAV. While in the previous section the sufficient distance seemed to change seemingly at random, inspecting the values listed in Table 2 reveals a pattern among the antenna systems of similar electrical size. For example, for *small systems* (AS1 and AS2) horizontal pattern observation, the sufficient distance needs to be significantly larger than the distance projected by (1). Consequently, the quadratic phase errors have to be significantly lower. Moreover, for both cases, the phase errors differ only by 2°. A similar situation occurs for the observation of vertical patterns. In the case of a *medium system* (AS3 – AS5), for the observation of horizontal pattern the quadratic phase error values are within 20 – 30°, which is very close the specification by (1). Similarly, for the vertical pattern observations the determined distances and phase errors are close to the (1), making it a good estimation of the sufficient measurement distance. The most varied appears to be the case of *large antenna systems*, especially between the sufficient distances for horizontal and vertical observations. Results suggest that horizontal pattern observations can be performed significantly closer than initially predicted, with phase error values reaching up to 177.7°. Conversely, vertical pattern observations must be conducted at much greater distances, with phase error values going as low as 3.9°. Furthermore, r_{1v} for AS6 and AS7 is greater than r_4, which means that vertical and horizontal pattern measurements could not be performed at the same distance. At the same time r_{1h} for AS8 is lower than both r_2 and r_4, meaning

Table 1: List of tested antenna systems

AS#	Largest dimension (D)	Projected centre frequency	Number of antenna levels	Number of antennas in a single level
AS1	5.69 m ≈ 2 λ | (small)	96.0 MHz	2	3
AS2	5.69 m ≈ 2 λ | (small)	97.5 MHz	2	3
AS3	12.1 m ≈ 4 λ | (medium)	97.5 MHz	4	3
AS4	12.1 m ≈ 4 λ | (medium)	97.5 MHz	4	2
AS5	12.1 m ≈ 4 λ | (medium)	100.0 MHz	4	4
AS6	24.89 m ≈ 8 λ | (large)	97.6 MHz	8	4
AS7	24.89 m ≈ 8 λ | (large)	92.5 MHz	8	3
AS8	3.3 m ≈ 7 λ | (large)	650.0 MHz	3	4

Table 2: List of sufficient far-field radiation pattern observation distances

AS#	r_{1h} in m	Δr_{1h} in m	ψ_h in °	r_{1v} in m	Δr_{1v} in m	ψ_v in °	r_2 in m
AS1	75	0.017λ	6.2	55	0.024λ	8.5	5.28
AS2	58	0.023λ	8.2	75	0.018λ	6.2	5.31
AS3	75	0.079λ	28.6	83	0.072λ	25.8	11.45
AS4	95	0.063λ	22.6	107	0.055λ	20.0	11.45
AS5	105	0.058λ	20.9	55	0.111λ	40.0	11.45
AS6	55	0.453λ	165.0	1 420	0.018λ	6.4	22.90
AS7	85	0.279λ	101.2	1 750	0.013λ	4.9	20.45
AS8	6	0.483λ	177.1	292	0.010λ	3.9	19.08

$r_3 = 18.18$ m

$r_4 = 500$ m

Table 3: General sufficient measurement distances.

	Horizontal	Vertical
Small AS | $D \leq 2.5\,\lambda$	$r_{1h} \geq \frac{7.5D^2}{\lambda}$	$r_{1v} \geq \frac{7.5\,D^2}{\lambda}$
Medium AS | $D \approx 4\,\lambda$	$r_{1h} \geq \frac{2.5\,D^2}{\lambda}$	$r_{1v} \geq \frac{2.5\,D^2}{\lambda}$
Large AS | $D \geq 7\,\lambda$	$r_{1h} \geq \frac{D^2}{2\,\lambda}$	$r_{1v} \geq \frac{12D^2}{\lambda}$

these criteria must be prioritized to ensure the quadcopter itself does not introduce significant measurement error.

Based on the results, general equations can be derived for horizontal and vertical pattern observations. These equations are displayed in Table 3.

4.1. Discussion

Results suggest that, while the widely utilized rule-of-thumb criterion for far-field radiation pattern measurements sets a good basis for the sufficient minimal distance estimation, it has been generalized over the years and applied even in cases where a strict compliance can lead to substantial systematic error. In the past, there was no need to reevaluate this criterion for airborne measurements due to helicopters inability to reach anywhere close to this distance. Hence, the criterion was always satisfied, and larger issue was posed by the interference with ground reflections. The derived equations in Table 3 in almost all cases result in larger minimal measurement distance than the Rayleigh distance with the only exception being the minimal distance for horizontal pattern measurement of the *large AS*. In the cases of AS6 and AS8 (see Table 2) the quadratic phase error can reach up to ~170° for the resulting amplitude error to reach 0.5 dB. To explain this phenomenon, horizontal patterns of these antenna systems must be investigated. Horizontal patterns are displayed in Figure 10, and one notable feature they have in common is that the patterns are almost omnidirectional with very slightly attenuated minima between visible lobes (2-3 dB). This is in contrast to the horizontal patterns of other tested antenna systems, all of which have at least one attenuated region, including the AS7, where the value of phase error has to reach significantly lower values. This suggests that the possibility of the radiation pattern shape playing an important role in determining the sufficient measurement distance, in addition to the antenna system size. This is further supported by additional investigation involving vertical patterns at the maxima of side lobes, or minima. Even though the vertical pattern is almost similar to the vertical pattern at the azimuth of the main lobe's maximum radiation, the amplitude error was smaller than the maximum error value at much larger distances. For example, if the vertical pattern of AS1 was tested at the azimuth of 20° (see the horizontal pattern in Figure 6a for reference), the minimal sufficient distance was 180 m, which can be approximately written as $18\,D^2/\lambda$. From this, if the measurement of the vertical pattern is performed at the azimuth different than the main lobe maximum, the distance criterion should be reevaluated, or the measurement distance should be equal to at least $16\,D^2/\lambda$. While for a *small AS* vertical flight at this distance can still be executed, the problem arises with the minimal sufficient distance for vertical pattern measurement of a *large AS*. According to the Table 2 the minimal sufficient observation distance is 1 750 m, and it would be even larger if the relation from Table 3 is observed.

Due to the pattern expanding with distance, at this distance, the quadcopter would have to cover approximately 1 000 m of vertical distance in order to encompass the main lobe and four sidelobes at each main lobe side which may not be possible to perform at some locations, and a rigorous survey of the surrounding terrain should be carried out prior to the measurements. Furthermore, the take-off point may have to be moved closer to the location of the vertical flight. As has already been established, with the utilized setup, horizontal pattern measurement cannot be carried out at similar distance, thus, either vertical and horizontal pattern measurements for the *large AS* will be performed at different distances, or a significant amplitude error in the vertical pattern data will have to be accepted.

Further motivation for performing horizontal pattern measurements as close as possible to the AS is due to the interference with the EM wave reflected from the ground. Horizontal patterns of AS1, calculated over an in-situ ground relief, are displayed in Figure 11. The horizontal pattern in Figure 11a, calculated at a distance of 170 m, already shows visible distortion due to ground reflections. In contrast, the horizontal pattern in Figure 11b, calculated at a distance of 300 m, barely resembles the original shape (Figure 6a). Thus, while in theory, and in free space, the farther the measurement is taken, the better; under real conditions the radiation pattern should be measured as close as possible to the AS, while avoiding unnecessary amplitude error.

A priori in-situ measurements conducted using the setup and procedure described in Section 2.2 are compared to the calculated vertical radiation pattern in cylindrical coordinates and are shown in Figure 12. The presented figures demonstrate good agreement between the shapes of measured and calculated vertical radiation patterns, especially in Figure 12b, where the main lobe width and sidelobe level are similar for both cases, despite the effects of the real environment during the measurement. It can therefore be expected that the

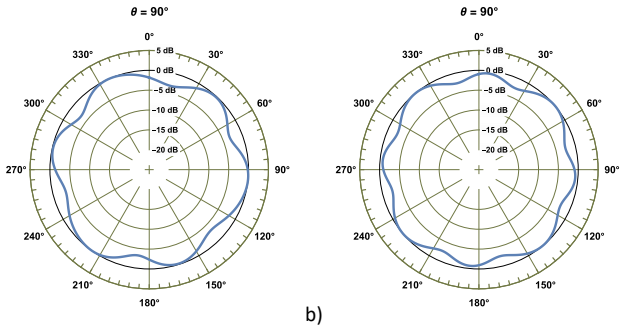

Figure 10: Radiation patterns in horizontal plane of: a) AS6, b) AS8.

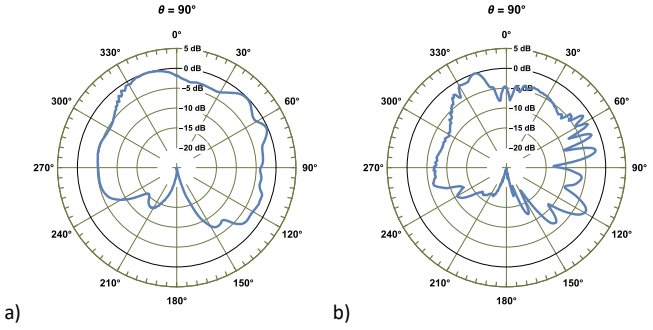

Figure 11: Radiation patterns in horizontal plane of AS1 calculated over the in-situ terrain at: a) 170 m, b) 300 m.

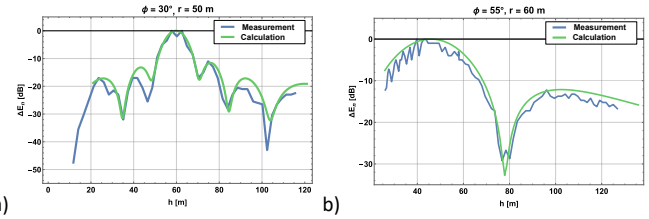

a) b)

Figure 12: Comparison of vertical pattern measurements with calculations for: a) AS5, b) AS1.

measurements of the other patterns presented in this study would also follow such a close correlation and can be considered valid estimations of the real radiation pattern behaviour. The successful implementation of the adjustments proposed in this study in real measurements would streamline the radiation pattern evaluation, making use of the enhanced capabilities and versatility provided by a UAV, such as a quadcopter. Nevertheless, additional calculations involving various antenna systems need to be performed, as well as measurements confirming the calculations, before final conclusions can be drawn. As demonstrated in Figure 11, quadratic phase error is not the only quantity influencing the airborne measurements. Therefore, measurement in controlled environment such as anechoic chamber with a scaled substitute AS, could provide more accurate results.

5. CONCLUSIONS

This study investigated the influence of the quadratic phase error on the resulting horizontal and vertical radiation patterns for large antenna systems. The presented results suggest that the widely used rule-of-thumb requirement for a minimal distance of $2D^2/\lambda$ is, in some cases, insufficient and, in others, overly restrictive. Eight antenna systems were tested in total, which were divided by the electrical size into *small, medium* and *large AS*. Sufficient measurement distances were determined based on the maximum amplitude error value of 0.5 dB. From the identified distances, general equations were derived for measurements of horizontal and vertical patterns for each AS group. For *small* and *medium antenna systems*, the defined equations specify larger measurement distance for both horizontal and vertical pattern measurements. Conversely, for *large AS* groups, shorter distance for horizontal pattern measurement was proposed. Thus, for the measurements of large antenna systems operating in the FM/DVB-T frequency bands, the minimal distance requirement may depend on the shape and taper of the radiation pattern in addition to the size of the AS itself. Additionally, this knowledge may not only streamline the airborne radiation pattern measurement but also can be beneficial for the diagnostics of the AS from radiation pattern measurements using a UAV, where distinct minima may appear if a faulty antenna is not radiating.

AUTHORS' CONTRIBUTION

J.K. – Conceptualization, Investigation, Data curation, Formal analysis, Methodology (FEKO calculations and distance investigation), Writing – original draft;
M.D. – Formal analysis, Investigation, Methodology (airborne measurement methodology);
R.H. – Conceptualization, Funding acquisition, Supervision, Validation;
J.H. – Project administration, Resources (obtaining vital documentation);
A.K. - Visualization, Writing – review & editing;
M.Š. – Investigation, Validation

ACKNOWLEDGEMENT

This work was supported by the grant agency APVV under a project number APVV-20-0042 "Microelectromechanical sensors with radio frequency data transmission" and by the project ENEFS 09I05-03-V02-00041 "Novel electrically enhanced wireless method for sensing of mechanical quantities. Special thanks also go to the company Towercom, a.s. for providing vital technical documentation.

REFERENCES

[1] M. Dzuris, R. Hartansky, Sensor of electromagnetic field for large antenna system measurement. (Senzor elektromagnetického poľa pre meranie veľkých anténnych systémov - original), Master thesis, Slovak University of Technology in Bratislava, Bratislava, 2022 [In Slovak].

[2] R. Palmeri, G.M. Battaglia, A. F. Morabito, S. Costanzo, F. Venneri, T. Isernia, Fault Diagnosis of Realistic Arrays from a Reduced Number of Phaseless Near-Field Measurements, in IEEE Transactions on Antennas and Propagation, vol. 71, n. 9, 2023, pp. 7206-7219.
DOI: 10.1109/TAP.2023.3293004

[3] P. Kopecky, V. Zavodny, Measurement of far-field patterns of phased array antennas, in 2015 Conference on Microwave Techniques (COMITE), 2015, pp. 1-3.
DOI: 10.1109/COMITE.2015.7120333

[4] B. Witvliet, Airborne evaluation/verification of antenna pattern of broadcasting stations, in 18th Int. Wroclaw symp. and exhibition on Electromagnetic compatibility, vol. 1, 2016, pp. 433-438.

[5] M. Dzuris, R. Hartansky, J. Krchnak, Measuring the radiation pattern of large FM antenna system, in Measurement 2023: 14th Int. conf. on Measurement, pp. 135-138, Slovak Academy of Sciences, 2023, Bratislava.
DOI: 10.23919/MEASUREMENT59122.2023.10164409

[6] F. Paonessa, G. Virone, E. Capello, G. Addamo, O. A. Peverini (+ 11 other authors), VHF/UHF antenna pattern measurement with unmanned aerial vehicles, IEEE Conf. Morphology for Aerospace (MetroAeroSpace), Florence, Italy, 22-23 June 2016, pp. 87-91.
DOI: 10.1109/MetroAeroSpace.2016.7573191

[7] A. N. Cadavid, J. Aristizabal, M. D. P. Alhucerna, Antenna pattern verification for Digital TV Broadcast systems in Andean countries based on UAVs, 2018 IEEE-APS Topical Conf. on Antennas and Propagation in Wireless Communications (APWC), Cartagena, Colombia, 2018, pp. 858-861.
DOI: 10.1109/ACCESS.2020.3027790

[8] A. Y. Umeyama, J. L. Salazar-Cerreno, C. J. Fulton, UAV-Based Far-Field Antenna Pattern Measurement Method for Polarimetric Weather Radars: Simulation and Error Analysis, in IEEE Access, vol. 8, 2020, pp. 191124-191137.
DOI: 10.1109/ACCESS.2020.3027790

[9] M. García-Fernández, Y. Á. López, A. Arboleya, B. González-Valdés, Y. Rodríguez-Vaqueiro + 2 other authors, Antenna Diagnostics and Characterization Using Unmanned Aerial Vehicles, in IEEE Access, vol. 5, 2017, pp. 23563-23575.
DOI: 10.1109/ACCESS.2017.2754985

[10] M. Heikkilä, M. Koskela, T. Kippola, M. Kocak, J. Erkkilä, J. Tervonen, Using Unmanned Aircraft Systems for Mobile Network Verifications, in IEEE 29th Annual International Symposium on Personal, Indoor and Mobile Radio Communications (PIMRC), Bologna, Italy, 2018, pp. 805-811.
DOI: 10.1109/PIMRC.2018.8580883

[11] Antenna measurements in VHF and UHF frequency bands (Měření antén v pásmu velmi krátkých a ultra krátkých vln - original), Federal Ministry of Transport and Communications. RA11 MDT 621.32, Approved by a decree FMDS 15434/89, 09.10.1989, Prague, Czechia, [In Czech].

[12] P. S. Hacker, H. E. Schrank, Range Distance Requirements for Measuring Low and Ultralow Sidelobe Antenna Patterns, IEEE Transactions on Antennas and Propagation, vol. AP-30, n. 5, 1982, pp. 956-966.
DOI: 10.1109/TAP.1982.1142916

[13] P. Corona, G. Ferrara, C. Gennarelli, Measurement distance requirements for both symmetrical and antisymmetrical aperture antennas, IEEE Transactions on Antennas and Propagation, vol. 37, n.8, 1989, pp. 990-995.
DOI: 10.1109/8.34135

[14] S. P. Skulkin, V. I. Turchin, N. I. Kascheev, Range distance Requirements for large antenna measurements for linear aperture with uniform field distribution, Progress in Electromagnetics Research M, Vol. 48, 2016. pp. 87-94.
DOI: 10.1109/LAWP.2018.2841645

[15] Report ITU-R SM.2056-1, Airborne verification of antenna patterns of broadcasting stations. Geneva: ITU – International Telecommunication Union, 2014.

[16] FEKO User's Manual. Suite 6.1, EM Software & Systems-S.A., (Pty) Ltd, 2011, 32 Techno Avenue, Technopark, Stekkenbosh, 7600, South Africa.

[17] Krchnak J., Hartansky R., Dzuris M., Stibrany M., Calculation of Induced Currents in Antenna System Anchoring Cables by Equivalent Source Substitution, in Measurement 2023: 14th Int. Conf. on Measurement, pp. 139-142.
DOI: 10.23919/MEASUREMENT59122.2023.10164480

[18] C. A. Balanis, Antenna Theory. Analysis and Design, 4th ed. John Wiley & Sons, Inc., New Jersey, 2015.

[19] J. Krchnak, R. Hartanský, M. Dzuris, J. Halgos, N. Grilli, M. Stibrany, Identification of Faulty Antenna in Large FM Antenna System Using Quadcopter Measurements, Int. Journal on Communications Antenna and Propagation, 13 (5) 2023, pp. 238-248.
DOI: 10.15866/irecap.v13i5.24214

[20] C. C. Cutler, A. P. King, W. E. Kock, Microwave Antenna Measurements, Proceeding of the I.R.E. December 1947, pp. 1462-1471.